Micellar lipid composition affects micelle interaction with class B scavenger receptor extracellular loops

Aurélie Goncalves, Brigitte Gontero, Marion Nowicki, Marielle Margier, Gabriel Masset, Marie Josephe Amiot-Carlin, Emmanuelle Reboul

Micellar lipid composition affects micelle interaction with class B scavenger receptor extracellular loops

Aurélie Goncalves,*,†,§ Brigitte Gontero,** Marion Nowicki,*,†,§ Marielle Margier,*,†,§ Gabriel Masset,*,†,§ Marie-Josèphe Amiot,*,†,§ and Emmanuelle Reboul[1],*,†,§

INRA,* UMR 1260 "Nutrition, Obesity and Risk of Thrombosis," F-13385 Marseille, France; INSERM,† UMR 1062, F-13385 Marseille, France; Aix-Marseille Université,§ F-13385 Marseille, France; and Aix-Marseille Université CNRS,** BIP, UMR 7281, F-13402 Marseille, France

Abstract Scavenger receptors (SRs) like cluster determinant 36 (CD36) and SR class B type I (SR-BI) play a debated role in lipid transport across the intestinal brush border membrane. We used surface plasmon resonance to analyze real-time interactions between the extracellular protein loops and various ligands ranging from single lipid molecules to mixed micelles. Micelles mimicking physiological structures were necessary for optimal binding to both the extracellular loop of CD36 (lCD36) and the extracellular loop of SR-BI (lSR-BI). Cholesterol, phospholipid, and fatty acid micellar content significantly modulated micelle binding to and dissociation from the transporters. In particular, high phospholipid micellar concentrations inhibited micelle binding to both receptors (-53.8 and -74.4% binding at 0.32 mM compared with 0.04 mM for lCD36 and lSR-BI, respectively, $P < 0.05$). The presence of fatty acids was crucial for micelle interactions with both proteins (94.4 and 81.3% binding with oleic acid for lCD36 and lSR-BI, respectively, $P < 0.05$) and fatty acid type substitution within the micelles was the component that most impacted micelle binding to the transporters. These effects were partly due to subsequent modifications in micellar size and surface electric charge, and could be correlated to micellar vitamin D uptake by Caco-2 cells. Our findings show for the first time that micellar lipid composition and micellar properties are key factors governing micelle interactions with SRs.—Goncalves, A., B. Gontero, M. Nowicki, M. Margier, G. Masset, M-J. Amiot, and E. Reboul. **Micellar lipid composition affects micelle interaction with class B scavenger receptor extracellular loops.** *J. Lipid Res.* 2015. **56:** 1123–1133.

Supplementary key words scavenger receptor class B type I • cluster determinant 36 • cholesterol • phospholipids • fatty acid • cholecalciferol • intestine • surface plasmon resonance

Scavenger receptors (SRs) such as cluster determinant 36 (CD36) and SR class B type I (SR-BI) are recognized to play a major role in lipid transport across cell membranes, although their function at the intestinal level is still a matter of debate.

CD36 is an 88 kDa transmembrane protein with broad specificity. It interacts with many ligands, including native and oxidized lipoproteins, long-chain fatty acids, cholesterol, anionic phospholipids, carotenoids, and vitamin D [for review see (1)], as well as vitamin K (2). CD36 is highly expressed in the proximal part of the intestine (duodenum and jejunum) (3), where it is assumed to play a key role in fatty acid (4) and cholesterol (5) uptake. Indeed, it has been demonstrated both in vitro and in vivo that isolated enterocytes or proximal intestine from CD36-null mice show reduced fatty acid uptake compared with wild-type mice (3) and that a CD36 deletion suppresses oleic acid (OA) uptake into the duodenum and reduces it in the jejunum of mice fed triolein (6). Similarly, CD36-deficient mice displayed an accumulation of dietary cholesterol in the intestinal lumen and a reduction of dietary cholesterol transport into the lymph (7). However, it was later shown that CD36 deletion in mice was not rate-limiting for cholesterol absorption (8). Moreover, it was suggested that the primary role of CD36 was not to mediate fatty acid but to promote the production of large triglyceride-rich lipoproteins (9, 10).

SR-BI is an 82 kDa transmembrane protein that interacts with an equally wide range of ligands such as HDL, anionic phospholipids, cholesterol, carotenoids, and vitamins D, E (1), and K (2). At the intestinal level, SR-BI was shown to facilitate the uptake of free cholesterol as well as esterified cholesterol, phospholipids, and triacylglycerol hydrolysis products (11, 12). However, the effective role of SR-BI compared with Niemann-Pick C1-like 1 in terms of cholesterol transport is still a matter of debate (8). It has

Abbreviations: aa, amino acid; ALA, α-linolenic acid; ARA, arachidonic acid; CD36, cluster determinant 36; LA, linoleic acid; lCD36, extracellular loop of cluster determinant 36; lSR-BI, extracellular loop of scavenger receptor class B type I; NTA, nitrilotriacetic acid; OA, oleic acid; PA, palmitic acid; RU, response unit; SPR, surface plasmon resonance; SR, scavenger receptor; SR-BI, scavenger receptor class B type I.
[1] To whom correspondence should be addressed.
  e-mail: Emmanuelle.Reboul@univ-amu.fr

recently been hypothesized that the main role of SR-BI was either to facilitate the uptake of other lipid molecules (1) or to mediate lipid sensing (13, 14), even if a significant involvement in lipid transport cannot be ruled out.

Numerous experiments on transfected cells have previously shown specific binding of lipoproteins, apolipoproteins, or phospholipids to SR-BI (15–17) or CD36 (18, 19), and there have been few attempts to investigate micellar cholesterol binding with one or both SRs at the intestinal level (13, 20, 21). However, the molecular functions of these two multiligand proteins leading to selective dietary lipid transport remain largely unclear. To gain insight into intestinal CD36 and SR-BI function, we used surface plasmon resonance (SPR) to analyze real-time interactions between the isolated extracellular protein loops (lSR-BI and lCD36) and various ligands ranging from single lipid molecules to mimetic physiological structures such as mixed micelles.

MATERIALS AND METHODS

Chemicals

Sodium taurocholate, free cholesterol, 2-oleoyl-1-palmitoyl-*sn*-glycero-3-phosphocholine (phospholipid), 1-palmitoyl-*sn*-glycero-3-phosphocholine (lysophospholipid), monoolein, OA, palmitic acid (PA), linoleic acid (LA), α-linolenic acid (ALA), arachidonic acid (ARA), *cis*-5,8,11,14,17-eicosapentaenoic acid (EPA), *cis*-4,7,10,13,16,19-docosahexaenoic acid (DHA), and vitamin D (cholecalciferol) were purchased from Sigma-Aldrich (Saint-Quentin-Fallavier, France). Nitrilotriacetic acid (NTA) sensor chips were purchased from GE Healthcare Life Sciences (Vélizy-Villacoublay, France). Recombinant human lSR-BI (proline 33 to tyrosine 443 from protein sequence NP_005496.4) and lCD36 (glycine 30 to asparagine 439 from protein sequence NP_001001547.1) fused with poly-histidine tag were purchased from Sino Biological Inc. (Beijing, China). The recombinant proteins were produced in human HEK cells, enabling: *i*) the formation of the disulfide bonds as previously described (22); and *ii*) an accurate glycosylation process as demonstrated by the molecular mass of the loops (75–92 kDa). Both parameters have been shown to be important to maintain the lipid-transporter activity of the proteins (22, 23).

ClustalW sequence alignment of the two recombinant proteins is presented in **Fig. 1**: the extracellular loops are represented with blue residues and the deleted amino acids (aas) are in gray. Recombinant His-tag CP12, used as a control protein for SPR experiment, was produced and purified as described previously (24).

Preparation of analyte solutions

Fatty acid solutions. Stock solutions of OA and DHA from 1 to 100 mM were prepared by dissolving an adequate quantity of each fatty acid in propan-1-ol. Ten microliters of each stock solution was diluted to 1 ml of running buffer [10 mM HEPES, 150 mM NaCl, 50 μM EDTA, 0.001% Chaps (pH 7.4)], then sonicated in a water bath for 10 min and vortexed to obtain homogeneous solubilization.


```
SRBI  MGCSAKARWAAGALGVAGLLCAVLGAVMIVMVPSLIKQQVLKNVRIDPSSLSFNMWKEIP  60
CD36  MGCDRNCGLIAG--AVIGAVLAVFGGILMPVGDLLIQKTIKKQVVLEEGTIAFKNWVKTG  58
      MGC. :.   AG  .V G : AV:G.::: :   LI:: : K:V :: .:::F: W :

SRBI  IPFYLSVYFFDVMNPSEILK-GEKPQVRERGPYVYR-EFRHKSNITFNNND-TVSFLEYR  117
CD36  TEVYRQFWIFDVQNPQEVMMNSSNIQVKQRGPYTYRVRFLAKENVTQDAEDNTVSFLQPN  118
      .Y ..::FDV NP.E::  ..: QV::RGPY.YR .F  K.N:T : :D TVSF: .

SRBI  TFQFQPSKSHGSESDYIVMPNILVLGAAVMMENKPMTLKLIMTLAFTTLGERAFMNRTVG  177
CD36  GAIFEPSLSVGTEADNFTVLNLAVAAASHIYQN--QFVQMILNSLINKSKSSMFQVRTLR  176
      F:PS S G:E:D :.: N: V .A: : :N   :::I:. :.. .  F  RT:

SRBI  EIMWGYKDPLVNLINKYFPGMFPFKDKFGLFAELNNSDSGLFTVFTGVQNISRIHLVDRKW  237
CD36  ELLWGYRDPFLSLVP------YPVTTTVGLFYPYNNTADGVYKVFNGKDNISKVAIIDTY  230
      E::WGY:DP::.L:      :P.. ..GLF  NN: .G:..VF.G :NIS:: ::D.:

SRBI  NGLSKVDFWHSDQCNMINGTSGQMWPPFMTPESSLEFYSPEACRSMKLMYKESGVFEGIP  297
CD36  KGKRNLSYWES-HCDMINGTDAASFPPFVEKSQVLQFFSSDICRSIYAVFESDVNLKGIP  289
      :G  ::.:W.S :C:MINGT.. :PPF: .. L:F:S.: CRS:  :::.. ::GIP

SRBI  TYRFVAPKTLFANGSIYPPNEGFCP------CLESGIQNVSTCRFSAPLFLSHPHFLNA  350
CD36  VYRFVLPSKAFASPVENPDNYCFCTEKIISKNCTSYGVLDISKCKEGRPVYISLPHFLYA  349
      .YRFV P.. FA.   P N FC.   C . G: ::S.C: . P:::S PHFL A

SRBI  DPVLAEAVTGLHPNQEAHSLFLDIHPVTGIPMNCSVKLQLSLYMKSVAGIGQTGKIEP-V  409
CD36  SPDVSEPIDGLNPNEEEHRTYLDIEPITGFTLQFAKRLQVNLLVKPSEKIQVLKNLKRNY  409
      .P ::E.: GL:PN:E H  :LDI.P:TG:.:: : :LQ:.L :K.  I    :::

SRBI  VLPLLWFAESGAMEGETLHTFYTQLVLMPKVMHYAQYVLLALGCVLLLVPVICQIRSQEK  469
CD36  IVPILWLNETGTIGDEKANMFRSQVTGKINLLGLIRMILLSVGVVMFVAFMISYCACRSK  469
      ::P:LW: E:G:: .E. : F :Q:.  :

SRBI  CYLFWSSSKKGSKDKEAIQAYSESLMTSAPKGSVLQEAKL  509
CD36  TIK-------------------------------------  472
```

Fig. 1. Sequence alignment of CD36 and SR-BI. ClustalW sequence alignment of the two proteins. Conserved residues between CD36 and SR-BI are presented on the third line. The recombinant proteins used for the binding studies are represented with blue residues. (The gray residues have been deleted and replaced by poly-histidine tags at the C terminus of the proteins). The transmembrane segments are highlighted in yellow, disulfide bridges are represented by a green junction between cysteines and N-glycosylation are in pink. Inset: Coomassie Blue gel of recombinant human SR-BI and CD36 extracellular loops.

Simple micelles. These micelles were prepared from a mix of one lipid and the bile salt (taurocholate). An appropriate volume of lipid (either cholesterol, phospholipid, or free fatty acid) was transferred to a glass bottle and carefully evaporated under nitrogen. The dried residue was solubilized in running buffer containing 5 mM taurocholate and vigorously mixed by sonication at 25 W (Branson 250W Sonifier, Danbury, CT) for 2 min. The mixture obtained was filtered using a 0.22 μm filter (Millipore, Molsheim, France).

Mixed micelles. Mixed micelles were prepared as previously described (25) to obtain the final following concentrations: 0.04 mM phosphatidylcholine, 0.16 mM lysophosphatidylcholine, 0.3 mM monoolein, 0.1 mM free cholesterol, 0.5 mM OA, and 5 mM taurocholate (reference condition). Minor modifications were made depending on analyses (either a change in cholesterol or phosphatidylcholine concentrations or a substitution of free fatty acid type).

To assess the effect of mixed micelle quantity on micelle interactions with lCD36 and lSR-BI, mixed micelles were prepared with 0.08 mM phosphatidylcholine, 0.32 mM lysophosphatidylcholine, 0.6 mM monoolein, 0.2 mM free cholesterol, 1 mM fatty acid, and 10 mM taurocholate, and progressively diluted. These micelle lots differed by their lipid concentrations from 0.55 to 2.2 mM.

For cell experiments, mixed micelles were enriched with 0.5 μM vitamin D.

Phosphatidylcholine and cholesterol content of the micelles was assessed using kits from Biolabo (Maisy, France) according to the manufacturer's instructions, and results showed that lipid loss induced by filtration was less than 5%.

Measurement of mixed micelle size and zeta potential

The intensity-weighted mean hydrodynamic radius (reflecting particle size) and zeta potential (reflecting the electric charge on the particle surface) of the micelles were determined by photon correlation spectroscopy at 25°C on a Zetasizer Nano Zs system (Malvern Instruments, Malvern, UK) immediately after preparation of the mixed micelles.

Coomassie Blue gel

Five micrograms of each protein were separated on a 10% acrylamide gel with a Page Ruler Prestained Protein Ladder Plus size marker (Fermentas, Thermo Scientific, France). The gel was stained during 3 h in a color bath (50% methanol, 40% water, 10% acetic acid, and 0.25% Coomassie Blue) then destained overnight with washing solution (67.5% water, 25% methanol, and 7.5% acetic acid) to assess protein purity (Fig. 1, inset).

SPR

Purified His-Tag lSR-BI, His-Tag lCD36, and His-Tag CP12 were coupled to a carboxymethyl dextran matrix preimmobilized with NTA (chip NTA, BiaCore) following the manufacturer's instructions.

The interactions of various lipids or lipid micelles with immobilized proteins (ligands) were studied in HEPES running buffer (pH 7.4), after a 20 μl/min injection of 120 s, using a BiaCore T100 apparatus (GE Healthcare Life Sciences).

Global fits of the exponential curves (sensorgrams) were performed using the Biacore T100 Evaluation software (v4.1.1). Analyte binding to the ligand during the injection phase was defined at 120 s as the association phase, or "binding" (R120). Then, when the injection was stopped and replaced by running buffer, the analyte started to dissociate. This was defined as the dissociation phase at 150 s after injection (R150). R120 thus represents the amount of analyte bound 120 s after the beginning of injection, and R150 represents the amount of analyte that remains bound to the protein 30 s after the end of the injection (i.e., 150 s after the beginning of injection). The period of time of 120 s was specifically chosen during preliminary tests because most of the sensorgrams reached steady state during injection at this time. The period of time of 30 s after the end of the injection, i.e., during the dissociation phase, was specifically chosen because the dissociation was not complete and there were still bound analytes on the ligand, allowing comparison between different analytes. This was the only way to analyze the data, as the molar concentration of micelles is not known and as micelles are a mixture of different components. Therefore, dissociation (kd) and association (ka) rate constants cannot be determined, but R120 and R150 are report points that allow comparison between different analytes.

Most SPR data came from three independent experiments performed on different chips in which the initial amount of protein fixed could vary substantially, leading to response unit (RU) variations. These data were thus presented as percentage of a reference value set at 100% rather than RU. The percentages of dissociation were calculated as follows: $(R120 - R150)/R120 \times 100$.

For single molecule binding (OA and DHA), values for the dissociation and association rate constants, ka and kd, and the response at equilibrium R_{eq} were determined using the Biacore software. R_{eq} was then plotted as a function of OA and DHA concentration noted [A] and fitted to a hyperbola using SigmaPlot software (v11): $R_{eq} = R_{max}[A]/(K_D + [A])$, where the equilibrium constant K_D is the dissociation constant (inverse of the association or affinity constant), [A] the analyte concentration, and R_{max} the maximal response.

Caco-2 cell culture

Caco-2 clone TC-7 cells were cultured in the presence of DMEM supplemented with 16% heat-inactivated FBS, 1% nonessential aa, and 1% antibiotics (complete medium), as previously described (26). Cells were seeded and grown on transwells for 21 days, as previously described (26), to obtain confluent and highly-differentiated cell monolayers. At 12 h prior to each experiment, the medium used in apical and basolateral chambers was a serum-free complete medium.

At the beginning of each experiment, cell monolayers were washed with 0.5 ml PBS. For uptake experiments, the apical side of the cell monolayers received mixed micelles containing 0.5 μM of vitamin D (whereas the other side received the serum-free complete medium). Cells were incubated for 60 min at 37°C, and media were harvested at the end of each experiment. Cells were washed twice in 0.5 ml ice-cold PBS to eliminate adsorbed vitamin D, then scraped and collected in 0.5 ml PBS. Absorbed vitamin D was estimated as vitamin D in scraped cells plus vitamin D in the basolateral side of the cell monolayer, if any (26–28).

Statistical analysis

Analysis by group. Results are expressed as means ± SD. Differences between more than two groups of unpaired data were tested by the nonparametric Kruskal-Wallis test. The nonparametric Mann-Whitney U test was used as a post hoc test when the Kruskal-Wallis test showed significant differences between groups. Differences between two groups of unpaired data were tested using the nonparametric Mann-Whitney U test. Correlations between two groups of paired data were tested using the nonparametric Spearman test. Values of $P < 0.05$ were considered significant. All statistical analyses were performed using Statview software, version 5.0 (SAS Institute, Cary, NC).

ANOVA. Associations between the lipid types (either cholesterol, phospholipid, or free fatty acid), hydrodynamic radius, zeta potential, and the binding and dissociation phases of lCD36 and lSR-BI were further assessed by univariate and multivariate

ANOVA using SAS software version 9.3 (SAS Institute). The multivariate model included the three lipid types (cholesterol, phospholipid, and free fatty acid) as explanatory variables; partial effect size and significance level were estimated using semi-partial Eta-square coefficient and type III sum of squares.

RESULTS

Effect of micellar lipid composition on micelle interactions with lCD36 and lSR-BI

Control experiments were performed with CP12, an 8.5 kDa nuclear-encoded chloroplast protein isolated from photosynthetic organisms and having no known lipid binding functionality. Sensorgrams obtained with the His-tagged protein from a green alga (blanks) showed no binding in any condition and did not differ from the sensorgrams obtained without protein (data not shown).

Protein purity of the SRs was first confirmed by Coomassie Blue gel (Fig. 1, inset). Typical SPR sensorgrams illustrating micelle binding with a SR are shown in **Fig. 2**. Micelle capacity to bind and to dissociate from either lSR-BI or lCD36 was dependent on their total lipid composition. Moreover, broad differences were observed between simple micelles containing cholesterol and taurocholate only, and more complex micelles made with a mixture of lipids as found in the gut lumen in postprandial conditions (i.e., mixed micelles composed of cholesterol, phospholipids, lysophospholipids, monoolein, OA, and taurocholate) (**Fig. 3**). The binding of the simple micelles to lCD36 and lSR-BI after a contact time of 120 s (R120) was 3.9-fold and 1.6-fold lower than the binding observed with the mixed micelles. Furthermore, percentage of dissociation at 150 s was drastically higher for simple micelles than mixed micelles: 85.0 and 76.3% of ligands dissociated from lCD36 and lSR-BI, respectively, with simple micelles versus 38.0 and 12.9% with mixed micelles (Fig. 3). Similar results were obtained using simple micelles composed with either 0.04 mM of phospholipid or 0.5 mM of OA and taurocholate (data not shown) compared with mixed micelles. These results indicated that the SRs have a better affinity for the mixed micelles than for the simple micelles. Consequently, mixed micelles were used as a model for the rest of the study.

Effect of mixed-micelle quantity on micelle interactions with lCD36 and lSR-BI

In order to understand whether the amount of ligands can impact their interaction with the proteins, we used a series of different micelle concentrations (Fig. 2). The data highlighted that micelle amount could significantly impact both binding to and dissociation from lCD36. Indeed, high micelle quantities induced a weaker interaction with lCD36 than small quantities. Micelle interactions with lSR-BI in similar conditions were comparable (data not shown). To understand this result, we assessed the effect of the dilution on mixed-micelle properties, i.e., micellar size and micellar surface electric charge (**Table 1**). Low lipid concentrations led to higher particle sizes than high lipid concentrations, and micelle size was significantly and positively correlated to both lCD36 R120 (Rho = 0.891, $P < 0.001$) and lSR-BI R120 (Rho = 0.825, $P < 0.001$), as well as to lCD36 R150 (Rho = 0.827, $P < 0.001$).

Effect of micellar cholesterol concentration on micelle interactions with lCD36 and lSR-BI

We then investigated the effect of cholesterol concentrations within the mixed micelles on micelle interactions with the SRs. The absence of cholesterol significantly decreased mixed-micelle binding to both lCD36 and lSR-BI, as the R120 was reduced by 25.4 and 35.78% compared with their respective control conditions (mixed micelles at 0.1 mM cholesterol; **Fig. 4**). The absence of cholesterol also increased mixed micelle dissociation from SR-BI. Percent dissociation was significantly higher without cholesterol ($83.5 \pm 28.6\%$ vs. $26.9 \pm 14.4\%$ in the control condition, $P < 0.05$). Concentrations higher than 0.1 mM significantly decreased micelle binding to lCD36 without affecting their ability to remain bound to the protein (Fig. 4A). In contrast, the increase in cholesterol concentration did not modify the R120 and therefore the same association for lSR-BI was obtained compared with controls, but
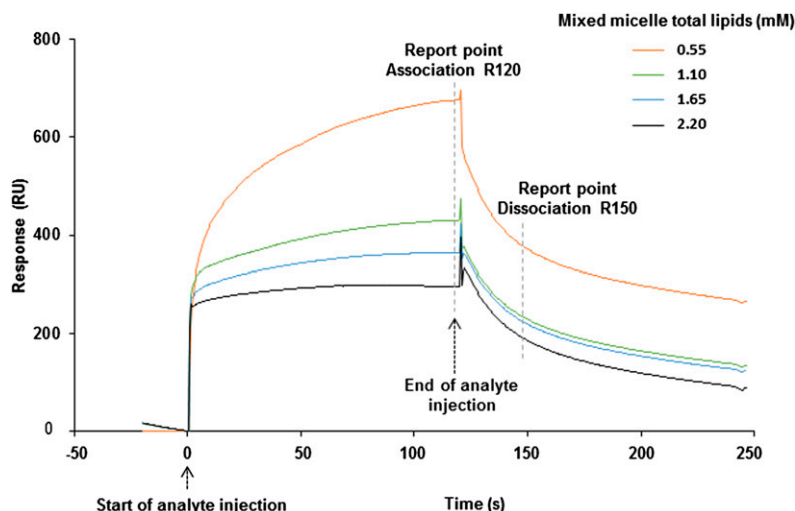

Fig. 2. Sensorgrams comparing abilities of mixed micelles at different dilutions to interact with CD36. Mixed micelles were prepared as described in the Material and Methods. The sensorgrams illustrate the interaction responses obtained when different dilutions of mixed micelles were injected over lCD36. Mixed micelles differed by their lipid concentrations from 0.55 to 2.2 mM. The landmarks used to compare binding (R120) and dissociation (R150) responses between two analytes are represented by a dashed line.
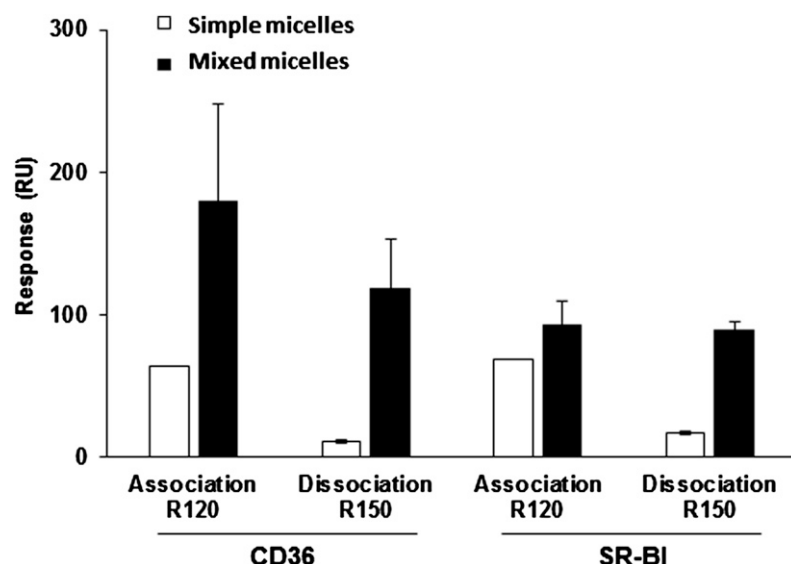
Fig. 3. Comparison between mixed micelle and cholesterol-taurocholate micelle interactions with lCD36 and lSR-BI. Mixed micelles (white bars) were composed of 0.5 mM OA, 0.16 mM lysophosphatidylcholine, 0.3 mM monoolein, 0.04 mM phosphatidylcholine, 0.1 mM cholesterol, and 5 mM taurocholate. Cholesterol-taurocholate micelles (simple micelles, black bars) were composed of 0.1 mM cholesterol and 5 mM taurocholate. Data are means ± SD of three assays with three independent micelle batches. Micelle binding (R120) and dissociation (R150) were measured as presented in the Material and Methods.

there was higher dissociation at 0.2 mM cholesterol (54.4 ± 5.0% vs. 26.9 ± 14.4% in the control condition, $P < 0.05$).

Effect of micellar phospholipid concentration on micelle interactions with lCD36 and lSR-BI

Micelle binding to lCD36 was significantly altered at high phospholipid concentrations (0.08–0.32 mM) but also when micellar composition was phospholipid-free (**Fig. 5A**). Increasing the phospholipid concentration resulted in a linear decrease in mixed-micelle binding to lSR-BI (Rho = −0.91, $P = 0.0007$; Fig. 5B). Interestingly, the percentages of micelles dissociated were increased for both SRs in the absence of phospholipid compared with the control condition (41.7 ± 20.7% vs. 27.1 ± 7.8% and 38.1 ± 8.0% vs. 16.3 ± 11.8% for lCD36 and lSR-BI, respectively), although the difference was only significant for lSR-BI.

Effect of micellar free fatty acid type on micelle interactions with lCD36 and lSR-BI

As shown in **Fig. 6**, the absence of fatty acid drastically decreased micelle binding to both lCD36 and lSR-BI

TABLE 1. Size and zeta potential of mixed micelles at various concentrations

Mixed Micelle Taurocholate Concentration (mM)	Mixed Micelle Lipid Concentration (mM)	Size (nm)	Zeta Potential (mV)
2.5	0.55	6.0 ± 1.6	−37.7 ± 3.0
3	0.66	6.7 ± 1.2[a]	−38.7 ± 3.4
4	0.88	5.0 ± 1.3	−37.2 ± 0.5
5 (control)	1.10	3.9 ± 1.1	−32.3 ± 4.0
6	1.32	3.5 ± 0.2	−36.7 ± 1.2
7	1.54	3.0 ± 0.0[a]	−28.9 ± 9.2
7.5	1.65	2.9 ± 0.3[a]	−38.5 ± 0.8[a]
8	1.76	3.1 ± 0.0[a]	−36.6 ± 1.5
9	1.98	2.7 ± 0.0[a]	−38.5 ± 0.1[a]
10	2.20	2.6 ± 0.1[a]	−34.1 ± 3.5

The intensity-weighted mean radius and the zeta potential of the mixed micelles at various dilutions were determined by photon correlation spectroscopy at 25°C. Data are means ± SD of three assays.
[a] A significant difference ($P < 0.05$) with the control (assay performed with mixed micelles at 5 mM taurocholate and 0.16 mM lysophosphatidylcholine, 0.3 mM monoolein, 0.04 mM phosphatidylcholine and 0.5 mM OA).
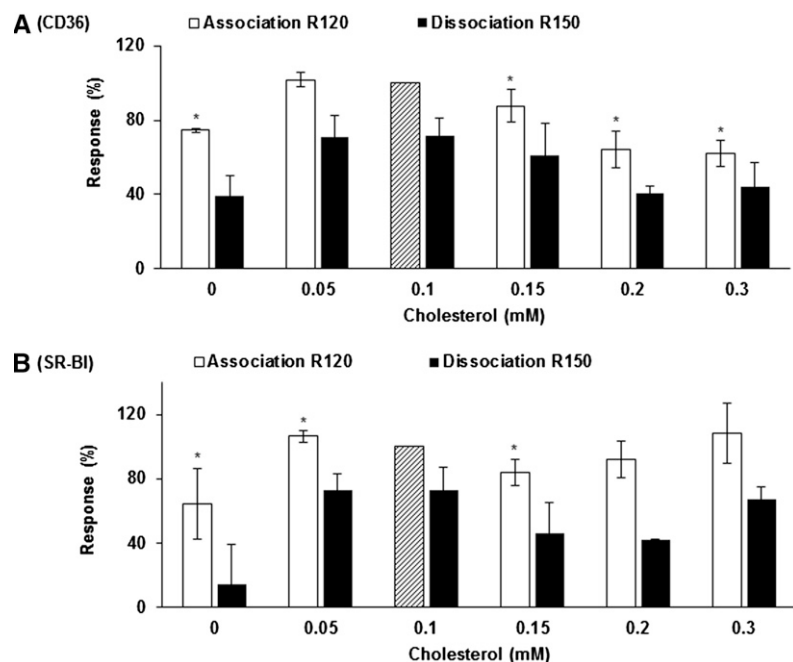
compared with OA micelles (−94.4 ± 9.7% and −81.3 ± 32.4%, respectively, $P < 0.05$). The presence of PA, LA, ALA, or EPA instead of OA also significantly decreased mixed micelle binding to both lCD36 and lSR-BI (up to −39%, $P < 0.05$). Interestingly, the presence of DHA significantly increased micelle binding to lCD36 compared with OA micelles. R150 analyses showed that micelles containing either LA, ALA, ARA, EPA, or DHA dissociated more rapidly from lCD36 than the micelles containing OA. Similarly, micelles containing either PA, ALA, or EPA dissociated more from SR-BI than the OA micelles. Our results thus highlighted that micelle binding to CD36 was positively correlated to both chain length (Rho = 0.73; $P = 0.0006$) and unsaturation (Rho = 0.60; $P = 0.0053$). Similarly, micelle binding to SR-BI was also positively correlated to both chain length (Rho = 0.58; $P = 0.0062$) and unsaturation (Rho = 0.45; $P = 0.0338$).

As OA and DHA appeared to increase micellar affinity for the SRs, we then determined their binding affinity constants with both lSR-BI and lCD36 using the single fatty acid. As molar concentrations were known, kinetic analysis was performed. The average apparent equilibrium dissociation constant (K_D) for OA was 349 ± 1 μM and 520 ± 2 μM for SR-BI and CD36, respectively. Surprisingly, the K_D for DHA was about 100-fold lower, at just 2.20 ± 0.01 μM and 3.20 ± 0.03 μM for lSR-BI and lCD36, respectively (**Fig. 7**).

ANOVA

Overall, univariate ANOVA (**Table 2**) first indicated that phospholipid concentration and fatty acid type, but not cholesterol concentration, impacted micellar electric charge (**Table 3**). Particle size (Table 3) was impacted by fatty acid type only (Table 2).

Univariate ANOVA also indicated that cholesterol and phospholipid concentrations, as well as free fatty acid type, were significantly correlated with both lCD36 and lSR-BI R120 and R150, explaining between 50 and 90% of the variance of levels. Particle size and surface electric charge were also moderately but significantly

Fig. 4. Effect of micellar cholesterol concentration on micelle interaction with lCD36 (A) and lSR-BI (B). All micelles were composed of 0.16 mM lysophosphatidylcholine, 0.3 mM monoolein, 0.04 mM phosphatidylcholine, 0.5 mM OA, and 5 mM sodium taurocholate. Cholesterol concentration ranged from 0 to 0.3 mM. Micelle binding (R120) and dissociation (R150) were measured according to the Material and Methods. Data are means ± SD of three assays on three different NTA chips with three independent micelle batches. An asterisk indicates a significant difference ($P < 0.05$) in binding compared with the control (mixed micelle at 0.1 mM of cholesterol standardized at 100%, hatched bar).

associated with lCD36 R120 and R150. Finally, micellar electric charge was modestly but significantly associated with lSR-BI binding and dissociation, whereas particle size had no effect.

Multivariate analysis (**Table 4**) then showed that free fatty acid type had the biggest effect on micellar electric charge, while both cholesterol concentration and type of free fatty acid were associated with particle size.

Association on (R120) and dissociation from (R150) lCD36 were more impacted by type of free fatty acid than by micellar cholesterol and phospholipid concentrations. In contrast, ligand dissociation from lSR-BI (R120) was mainly affected by phospholipid concentration and fatty acid type, while the dissociation process (R150) was more affected by cholesterol concentration and free fatty acid type than by phospholipid concentration.

Effect of micellar lipid content on vitamin D uptake by Caco-2 cells

The different mixed micelle lots were enriched with 0.5 μM vitamin D, and vitamin D uptake was assayed in Caco-2 differentiated monolayers. Results showed that cholesterol, phospholipids, and fatty acid micellar content significantly impacted vitamin D uptake by cells (**Fig. 8**). In particular, vitamin D uptake was decreased by high phospholipid (up to 69%, $P < 0.05$) and cholesterol (up to 61%, $P < 0.05$) micellar concentrations. It was also impaired in the presence of very long chain polyunsaturated fatty acids compared with OA (-7, -19, and -20% with ARA, EPA, and DHA, respectively; $P < 0.05$). When phospholipid micellar content was modulated, vitamin D uptake was positively correlated to lSR-BI R120 (Rho = 0.906, $P = 0.0007$). It was also positively correlated to R150
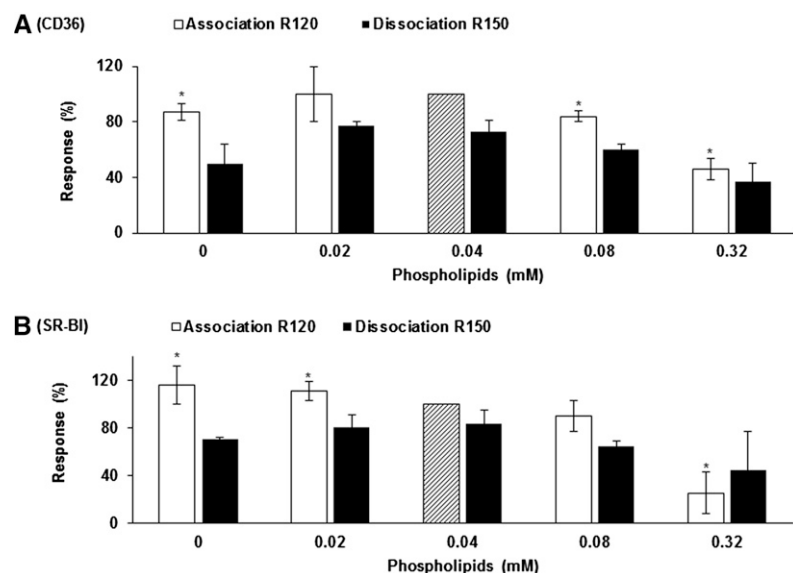

Fig. 5. Effect of micellar phospholipid concentration on mixed-micelle interactions with lCD36 (A) and lSR-BI (B). All micelles were composed of 0.16 mM lysophosphatidylcholine, 0.3 mM monoolein, 0.1 mM cholesterol, 0.5 mM OA, and 5 mM sodium taurocholate. Phospholipid concentration ranged from 0 to 0.32 mM. Micelle binding (R120) and dissociation (R150) were measured according to the Material and Methods. Data are means ± SD of three assays on three different NTA chips with three independent micelle batches. An asterisk indicates a significant difference ($P < 0.05$) compared with the control (mixed micelle at 0.04 mM of phospholipid standardized at 100%, hatched bar).
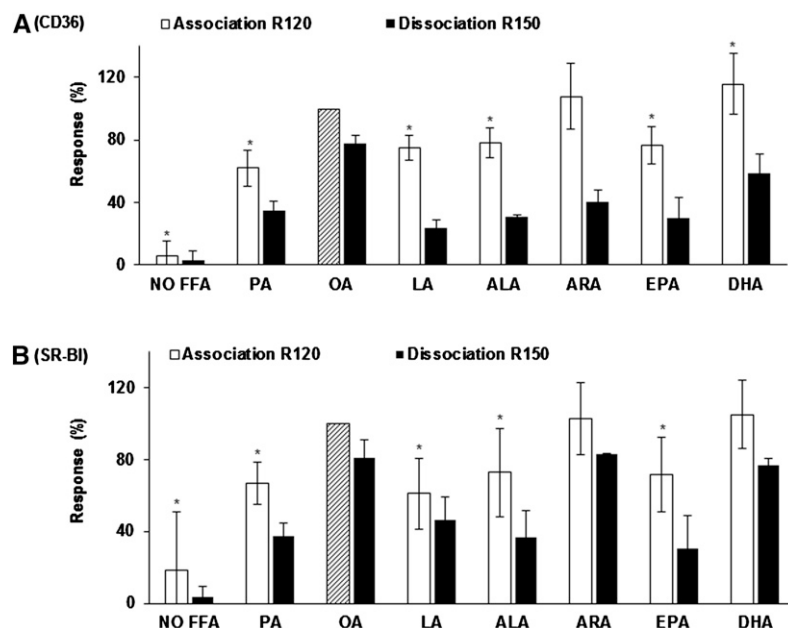
Fig. 6. Effect of micellar free fatty acid type on mixed-micelle interactions with lCD36 (A) and lSR-BI (B). All mixed micelles were composed of 0.16 mM lysophosphatidylcholine, 0.3 mM monoolein, 0.04 mM phosphatidylcholine, 0.1 mM cholesterol, and 5 mM sodium taurocholate. Only the free fatty acid composition differed between the different conditions: no free fatty acid or 0.5 mM of either PA, OA, LA, ALA, ARA, EPA, or DHA. Micelle binding (R120) and dissociation (R150) were measured according to the Material and Methods. Data are means ± SD of three assays on three different NTA chips with three independent micelle batches. An asterisk indicates a significant difference ($P < 0.05$) compared with the control (mixed micelle with OA standardized at 100%, hatched bar).

(Rho = 0.666, P = 0.0128). This suggested that the more the micelles were binding to lSR-BI, the higher was the uptake of vitamin D. When cholesterol or fatty acid micellar content was modified, vitamin D uptake was negatively correlated to lSR-BI R120 (Rho = −0.461, P = 0.0478; Rho = −0.489, P = 0.0191; for cholesterol and fatty acids, respectively). This suggested that the more the micelles were binding to lSR-BI, the lower was the uptake of vitamin D, and likely highlighted a competition between vitamin D and cholesterol or fatty acids as SR-BI ligands.

DISCUSSION

The molecular mechanisms underpinning the interaction between mixed micelles and the SRs CD36 and SR-BI at the brush border membrane level are poorly understood. Here, the SPR technique was used for the first time to detect real-time molecular interactions between mobile complex lipid structures, i.e., micelles, and the immobilized extracellular loop of CD36 and SR-BI. Because this methodology strictly detects mass, there is no need to label the interacting components, thus ruling out potential alterations of their molecular properties. We used SR extracellular loops and not entire proteins in order to avoid solubility issues as well as nonspecific binding of the hydrophobic analytes to the transmembrane domains of the proteins. The extracellular loops of SR-BI and CD36 represent 81 and 87% of the proteins (419 and 409 aas), respectively. The deletion of the two transmembrane domains (20 and 19 aas for SR-BI; 23 and 24 aas for CD36) and of the intracellular domains (12 and 37 aas for SR-BI; 6 and 9 aas for CD36) may impact the protein functioning. However, a recent work showed that critical subdomains for receptor-ligand interactions and transport function of SR-BI were located in the extracellular domain (29).

Mixed micelles were formulated in order to mimic physiological conditions and to represent lipid ratios that can be found in the human duodenum (i.e., total bile acid ~5–10 mM; cholesterol/lysophospholipids ~0.5 mM; cholesterol/monoglycerides ~0.4 mM) (25, 30), as well as to form micelles mainly according to photon correlation spectroscopy data. Sodium taurocholate appears to continuously self-aggregate over a large range of concentration (31), but a critical step of aggregation was shown to occur around 2–2.5 mM in the running buffer as well as in DMEM (data not shown), according to previous report (32). In the presence of lipids, such as lysophospholipids, critical micellar concentration is usually further reduced (33). These data support our observation that in our conditions, the mixture taurocholate-lipids is mainly present as micelles. These micelles were stable for several hours at room temperature, as determined by photon correlation spectroscopy (data not shown).
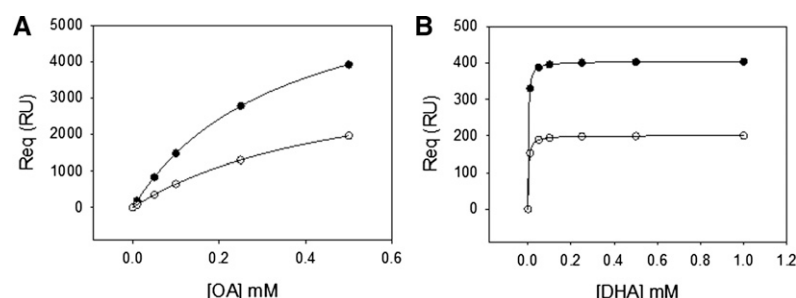

Fig. 7. Determination of binding affinity constants (K_D) by nonlinear regression fitting of a one-site binding model to the SPR data. Fatty acid propan-1-ol solutions from 0.01 to 1 mM were prepared by dissolving 1% of propan-1-ol containing an adequate quantity of fatty acid in running buffer. A: Response at equilibrium (R_{eq}) of OA with lCD36 and lSR-BI. B: Response at equilibrium (R_{eq}) of DHA with lCD36 and lSR-BI affinity. Filled circles, SRB1; open circles, CD36.

Micelle interaction with scavenger receptors   1129

TABLE 2. Univariate ANOVA

| | | | | Dependent Variables, Model R^2 | | | |
| | | | | lCD36 | | lSR-BI | |
Explanatory Variable	N	Zeta	Size	R120	R150	R120	R150
Cholesterol (Fig. 4)	18	0.17	0.62	0.91^a	0.67^c	0.66^c	0.75^b
Phospholipids (Fig. 5)	15	0.72^b	0.42	0.85^a	0.78^b	0.91^a	0.52
Fatty acids (Fig. 6)	24	0.79^a	0.74^b	0.90^a	0.92^a	0.72^b	0.90^a
Zeta (Table 3)	57	—	0.03	0.17^b	0.12^c	0.11^c	0.01
Size (Table 3)	57	0.03	—	0.25^a	0.10^c	0.03	0.08

The intensity-weighted mean radius and the zeta potential of the mixed micelles were determined by photon correlation spectroscopy at 25°C. Micelle binding (R120) and dissociation (R150) were measured as presented in the Material and Methods. Results expressed in R-square, e.g., 17% of the variation of zeta was explained by the variation of cholesterol concentration in the micelles.

^{a}$P < 0.001$.
^{b}$P < 0.01$.
^{c}$P < 0.05$.

A key finding is that these structures mimicking mixed micelles, i.e., including various lipids and lipid digestion products, are necessary for optimal binding to both lCD36 and lSR-BI. This is consistent with previous results showing that SR-BI could bind postprandial but not interprandial micelles (13), and that cholesterol uptake from simple micelles was unaffected by the addition of SR-BI inhibitor, in contrast to cholesterol uptake from mixed micelles (34).

To more specifically evaluate the effect of micellar lipid composition on micelle binding to the SRs, we first modulated their cholesterol content, as both proteins may participate partly in cholesterol transport (3, 12). Mixed-micelle binding to SR-BI was not modified within a wide

TABLE 3. Size and zeta potential of mixed micelles depending on their lipid content

		Size (nm)	Zeta Potential (mV)
Micellar	0	$4.4 ± 0.4^a$	$-38.2 ± 0.9^a$
cholesterol (mM)	0.05	$5.3 ± 1.1^a$	$-32.3 ± 4.0$
	0.1 (control)	$3.4 ± 0.1$	$-35.1 ± 1.8$
	0.15	$6.1 ± 0.5^a$	$-30.3 ± 4.5$
	0.2	$34.4 ± 23.3^a$	$-35.5 ± 1.3$
	0.3	$28.2 ± 7.2^a$	$-35.5 ± 1.8$
Micellar	0	$4.2 ± 0.4$	$-35.9 ± 1.3$
phospholipids (mM)	0.02	$4.6 ± 1.2$	$-28.2 ± 3.0^a$
	0.04 (control)	$3.8 ± 0.5$	$-37.4 ± 1.1$
	0.08	$4.8 ± 1.0$	$-34.5 ± 3.6$
	0.32	$6.8 ± 1.9^a$	$-31.2 ± 2.7^a$
Fatty acids	0	$28.8 ± 16.5^a$	$-14.8 ± 1.1^a$
	PA	$5.1 ± 1.7$	$-35.5 ± 4.5$
	OA (control)	$3.9 ± 0.9$	$-37.2 ± 2.3$
	LA	$3.5 ± 1.6$	$-30.2 ± 2.8^a$
	ALA	$2.8 ± 0.1^a$	$-29.6 ± 2.5^a$
	ARA	$3.6 ± 1.5$	$-30.9 ± 5.6$
	EPA	$3.8 ± 1.1$	$-26.9 ± 5.9^a$
	DHA	$3.9 ± 1.8$	$-29.7 ± 4.5^a$

Mixed micelles were composed of 5 mM taurocholate, 0.16 mM lysophosphatidylcholine, 0.3 mM monoolein, 0.04 mM phosphatidylcholine or another phosphatidylcholine concentration if indicated, 0.1 mM cholesterol or another cholesterol concentration if indicated, and 0.5 mM OA or another fatty acid if indicated. The intensity-weighted mean radius and the zeta potential of the mixed micelles were determined by photon correlation spectroscopy at 25°C. Data are means ± SD of three assays.

^{a}A significant difference ($P < 0.05$) with the control for each set of experiments.

range of cholesterol concentrations, whereas micelle binding to CD36 was optimal for a cholesterol concentration of around 0.1 mM. This suggests a complementary role of the two proteins during the digestion process, depending on micellar lipid composition. The interaction of micellar cholesterol with brush border membrane vesicles has been previously studied (20). The authors showed that although Niemann-Pick C1-like 1 has been described as the key mediator of intestinal cholesterol uptake, the active micelle binding was mediated by SR-BI, according to results obtained in Caco-2 cells (13). Here, the fact that both lSR-BI and lCD36 could efficiently bind mixed micelles is consistent with these data.

We then explored the effect of modulating micellar phosphatidylcholine concentrations on micelle interactions with the transporter extracellular loops. Both SR-BI and CD36 were primarily shown to be receptors for anionic phospholipids such as phosphatidylserine, but not for phosphatidylcholine (35). The specific binding of phosphatidylserine compared with other phospholipids was confirmed later by a solid-phase assay using lipid-coated plates (36). Our data, which show a decrease in micelle-SR loop interaction when phosphatidylcholine micellar content was increased, are in agreement with these results. Moreover, it has been clearly shown by several teams that phospholipids can impair the intestinal absorption of cholesterol or other lipid micronutrients [for review see (1)]. The inhibitory effect of phospholipids on other micellar lipid absorption may be due to a decrease in micellar affinity for their membrane transporters, as high micellar phospholipid concentrations inhibited micelle binding to both SR-BI and CD36 extracellular loops.

We also explored the effect of modulating micellar fatty acid type on micelle interactions with the SR loops and showed that free fatty acids were fundamental components of the structure. Interestingly, micelle binding to both transporters was positively correlated to chain length and unsaturation. This is in line with the concept of long-chain fatty acids being CD36 ligands (37). Moreover, accordingly to our SPR data showing that free OA and DHA were SR-BI ligands, mice overexpressing SR-BI at the

TABLE 4. Multivariate ANOVA

Model (N = 57)	Zeta	Size	lCD36		lSR-BI	
			R120	R150	R120	R150
All data (R^2)	0.62^a	0.70^a	0.90^a	0.86^a	0.80^a	0.81^a
Eta-square coefficient						
Cholesterol	0.08	0.38^a	0.15^a	0.20^a	0.08^c	0.31^a
Phospholipids	0.08	0.0	0.18^a	0.16^a	0.32^a	0.08^b
Fatty acids	0.51^a	0.29^b	0.69^a	0.62^a	0.39^a	0.54^a

The intensity-weighted mean radius and the zeta potential of the mixed micelles were determined by photon correlation spectroscopy at 25°C. Micelle binding (R120) and dissociation (R150) were measured as presented in the Material and Methods. Data of the complete model are expressed in R-square, i.e., 62% of the variation of zeta was explained by the combined effect of cholesterol concentration, phospholipid type, and fatty acid composition in the micelles. Eta-square coefficient corresponds to the semi partial effect of either cholesterol, phospholipids, or fatty acids in the model, i.e., adjusted for variations of the two other explanatory factors.
$^a P< 0.001.$
$^b P< 0.01.$
$^c P< 0.05.$

intestinal level displayed an increased uptake of labeled fatty acids compared with wild-type mice (12).

Overall, the lipid composition of mixed micelles clearly affects their ability to interact with the extracellular loops of both SRs. However, this is not the only parameter playing a key role in such an interaction. Univariate and mul-tivariate analysis of all experiments showed that surface electric charge of the mixed micelles, and to a lesser extent micellar size, impacted micelle interactions with the SR loops. This is consistent with new data on CD36 and SR-BI structures that recently emerged from the crystallization of another SR family member, lysosomal integral membrane
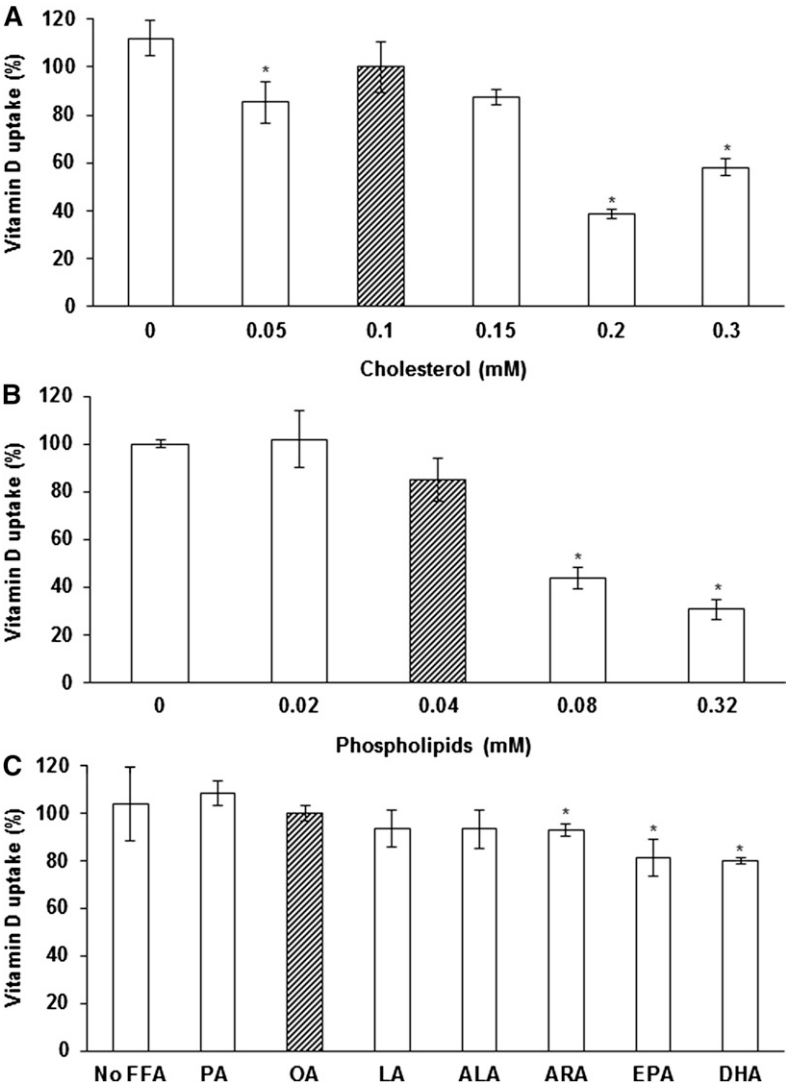

Fig. 8. Effect of lipid micellar content on vitamin D uptake by Caco-2 cells. The apical sides were incubated for 60 min with synthetic mixed micelles enriched with 0.5 μM cholecalciferol. The basolateral sides received FBS-free medium. Data are means ± SD of three assays. An asterisk indicates a significant difference (P < 0.05) with the controls (hatched bars). A: Effect of micellar phospholipid concentration. B: Effect of micellar cholesterol concentration. C: Effect of fatty acid substitution.

protein II (LIMPII) (38). The authors showed that the helical bundle face and the apex region forming the head of both proteins were important for ligand binding. We suggest that optimally sized structures would bind more efficiently to this specific area than other structures. Moreover, it was also shown that the apex regions of both human SR-BI and CD36 show a significant accumulation of cationic residue (38). An electrostatic interaction at the apex thus likely contributes to the binding of these receptors to their ligands. Mixed micelles being negatively charged, modifications in their lipid composition induce surface electric charge variations that may participate in the modulation of their binding to and dissociation from the SRs.

In order to correlate our SPR data with results in living cells, we performed micellar vitamin D uptake experiment in Caco-2 cells. These cells were specifically chosen because: *i*) they are resistant mixed micelles (unlike other cell types such as HEK or CHO cells, cytotoxicity tests not shown); *ii*) they highly express SR-BI and do not express CD36 (25); and *iii*) micelle binding to their apical membranes is SR-BI-dependent (20). Vitamin D uptake was significantly correlated with micelle binding to SR-BI. In particular, vitamin D uptake diminished with increasing micellar phospholipid contents, in accordance with the observation that phospholipids inhibit micelle association to SR-BI. Vitamin D uptake also diminished with increasing micellar cholesterol content, and it was negatively correlated to micelle binding to SR-BI. This likely reflects the fact that cholesterol is a good ligand for SR-BI that directly competes with vitamin D for uptake (38). Similarly, vitamin D uptake also diminished when very long chain fatty acids were substituted to OA and it was negatively correlated to micelle binding to SR-BI again. This is in agreement with our SPR data showing that long chain fatty acids like DHA are better ligands for SR-BI than OA and DHA may compete with vitamin D for uptake/binding.

Our SPR model presents several limits. First, this is an artificial system and extrapolations to physiological observations should be precautious. Second, the unstirred water monolayer of the brush border membrane cannot be modeled. Third, the use of a single protein does not represent full complexity of the brush border membrane surface, and so any possible cooperation between two or more membrane proteins can be evaluated. However, the SRP technique allowed the molecular interactions occurring between mixed micelles and intestinal SR extracellular loops to be characterized for the first time. The use of complex structures is particularly relevant regarding this type of study. Indeed, when OA or DHA was injected alone, the K_D of DHA for the receptors was about 100-fold smaller than the K_D of OA, showing that isolated molecules behave very differently from molecules incorporated in a physiological vehicle. However, it is noteworthy that both K_Ds were under the range of concentrations of fatty acids found in the gut (30). The smaller K_D of DHA compared with the K_D of OA was also in concordance with the reduced intake of polyunsaturared n-3 compared with monounsaturated fatty acids (39).

Further investigations on micelle binding to other intestinal lipid transporters are crucial in order to understand the full process of the binding of micellar structure to the enterocyte apical membrane. Further work is also necessary to evaluate other luminal lipid vehicles [vesicles, proteins, etc. (1)] binding to the membrane transport proteins.

Overall, our results show for the first time that the extracellular loops of CD36 and SR-BI are efficient receptors for intestinal mixed micelles. We also demonstrate that micellar lipid composition and micellar properties such as size and electric charge of the particles are key factors governing micelle interactions with intestinal SRs.

REFERENCES

1. Reboul, E., and P. Borel. 2011. Proteins involved in uptake, intracellular transport and basolateral secretion of fat-soluble vitamins and carotenoids by mammalian enterocytes. *Prog. Lipid Res.* **50:** 388–402.

2. Goncalves, A., M. Margier, S. Roi, X. Collet, I. Niot, P. Goupy, C. Caris-Veyrat, and E. Reboul. 2014. Intestinal scavenger receptors are involved in vitamin K1 absorption. *J. Biol. Chem.* **289:** 30743–30752.

3. Nassir, F., B. Wilson, X. Han, R. W. Gross, and N. A. Abumrad. 2007. CD36 is important for fatty acid and cholesterol uptake by the proximal but not distal intestine. *J. Biol. Chem.* **282:** 19493–19501.

4. Lobo, M. V., L. Huerta, N. Ruiz-Velasco, E. Teixeiro, P. de la Cueva, A. Celdran, A. Martin-Hidalgo, M. A. Vega, and R. Bragado. 2001. Localization of the lipid receptors CD36 and CLA-1/SR-BI in the human gastrointestinal tract: towards the identification of receptors mediating the intestinal absorption of dietary lipids. *J. Histochem. Cytochem.* **49:** 1253–1260.

5. Werder, M., C. H. Han, E. Wehrli, D. Bimmler, G. Schulthess, and H. Hauser. 2001. Role of scavenger receptors SR-BI and CD36 in selective sterol uptake in the small intestine. *Biochemistry.* **40:** 11643–11650.

6. Schwartz, G. J., J. Fu, G. Astarita, X. Li, S. Gaetani, P. Campolongo, V. Cuomo, and D. Piomelli. 2008. The lipid messenger OEA links dietary fat intake to satiety. *Cell Metab.* **8:** 281–288.

7. Nauli, A. M., F. Nassir, S. Zheng, Q. Yang, C. M. Lo, S. B. Vonlehmden, D. Lee, R. J. Jandacek, N. A. Abumrad, and P. Tso. 2006. CD36 is important for chylomicron formation and secretion and may mediate cholesterol uptake in the proximal intestine. *Gastroenterology.* **131:** 1197–1207.

8. Nguyen, D. V., V. A. Drover, M. Knopfel, P. Dhanasekaran, H. Hauser, and M. C. Phillips. 2009. Influence of class B scavenger receptors on cholesterol flux across the brush border membrane and intestinal absorption. *J. Lipid Res.* **50:** 2235–2244.

9. Tran, T. T., H. Poirier, L. Clement, F. Nassir, M. M. Pelsers, V. Petit, P. Degrace, M. C. Monnot, J. F. Glatz, N. A. Abumrad, et al. 2011. Luminal lipid regulates CD36 levels and downstream signaling to stimulate chylomicron synthesis. *J. Biol. Chem.* **286:** 25201–25210.

10. Masuda, D., K. Hirano, H. Oku, J. C. Sandoval, R. Kawase, M. Yuasa-Kawase, Y. Yamashita, M. Takada, K. Tsubakio-Yamamoto, Y. Tochino, et al. 2009. Chylomicron remnants are increased in the postprandial state in CD36 deficiency. *J. Lipid Res.* **50:** 999–1011.

11. Hauser, H., J. H. Dyer, A. Nandy, M. A. Vega, M. Werder, E. Bieliauskaite, F. E. Weber, S. Compassi, A. Gemperli, D. Boffelli, et al. 1998. Identification of a receptor mediating absorption of dietary cholesterol in the intestine. *Biochemistry.* **37:** 17843–17850.

12. Bietrix, F., D. Yan, M. Nauze, C. Rolland, J. Bertrand-Michel, C. Comera, S. Schaak, R. Barbaras, A. K. Groen, B. Perret, et al. 2006. Accelerated lipid absorption in mice overexpressing intestinal SR-BI. *J. Biol. Chem.* **281:** 7214–7219.

13. Béaslas, O., C. Cueille, F. Delers, D. Chateau, J. Chambaz, M. Rousset, and V. Carrière. 2009. Sensing of dietary lipids by enterocytes: a new role for SR-BI/CLA-1. *PLoS ONE.* **4:** e4278.

14. Saddar, S., V. Carriere, W. R. Lee, K. Tanigaki, I. S. Yuhanna, S. Parathath, E. Morel, M. Warrier, J. K. Sawyer, R. D. Gerard, et al.

2013. Scavenger receptor class B type I is a plasma membrane cholesterol sensor. *Circ. Res.* **112:** 140–151.

15. Acton, S., A. Rigotti, K. T. Landschulz, S. Xu, H. H. Hobbs, and M. Krieger. 1996. Identification of scavenger receptor SR-BI as a high density lipoprotein receptor. *Science.* **271:** 518–520.

16. Williams, D. L., M. de La Llera-Moya, S. T. Thuahnai, S. Lund-Katz, M. A. Connelly, S. Azhar, G. M. Anantharamaiah, and M. C. Phillips. 2000. Binding and cross-linking studies show that scavenger receptor BI interacts with multiple sites in apolipoprotein A-I and identify the class A amphipathic alpha-helix as a recognition motif. *J. Biol. Chem.* **275:** 18897–18904.

17. Thuahnai, S. T., S. Lund-Katz, D. L. Williams, and M. C. Phillips. 2001. Scavenger receptor class B, type I-mediated uptake of various lipids into cells. Influence of the nature of the donor particle interaction with the receptor. *J. Biol. Chem.* **276:** 43801–43808.

18. Calvo, D., D. Gomez-Coronado, Y. Suarez, M. A. Lasuncion, and M. A. Vega. 1998. Human CD36 is a high affinity receptor for the native lipoproteins HDL, LDL, and VLDL. *J. Lipid Res.* **39:** 777–788.

19. Tait, J. F., and C. Smith. 1999. Phosphatidylserine receptors: role of CD36 in binding of anionic phospholipid vesicles to monocytic cells. *J. Biol. Chem.* **274:** 3048–3054.

20. Labonté, E. D., P. N. Howles, N. A. Granholm, J. C. Rojas, J. P. Davies, Y. A. Ioannou, and D. Y. Hui. 2007. Class B type I scavenger receptor is responsible for the high affinity cholesterol binding activity of intestinal brush border membrane vesicles. *Biochim. Biophys. Acta.* **1771:** 1132–1139.

21. van Bennekum, A., M. Werder, S. T. Thuahnai, C. H. Han, P. Duong, D. L. Williams, P. Wettstein, G. Schulthess, M. C. Phillips, and H. Hauser. 2005. Class B scavenger receptor-mediated intestinal absorption of dietary beta-carotene and cholesterol. *Biochemistry.* **44:** 4517–4525.

22. Yu, M., T. Y. Lau, S. A. Carr, and M. Krieger. 2012. Contributions of a disulfide bond and a reduced cysteine side chain to the intrinsic activity of the high-density lipoprotein receptor SR-BI. *Biochemistry.* **51:** 10044–10055.

23. Viñals, M., S. Xu, E. Vasile, and M. Krieger. 2003. Identification of the N-linked glycosylation sites on the high density lipoprotein (HDL) receptor SR-BI and assessment of their effects on HDL binding and selective lipid uptake. *J. Biol. Chem.* **278:** 5325–5332.

24. Graciet, E., P. Gans, N. Wedel, S. Lebreton, J. M. Camadro, and B. Gontero. 2003. The small protein CP12: a protein linker for supramolecular complex assembly. *Biochemistry.* **42:** 8163–8170.

25. Reboul, E., L. Abou, C. Mikail, O. Ghiringhelli, M. Andre, H. Portugal, D. Jourdheuil-Rahmani, M. J. Amiot, D. Lairon, and P. Borel. 2005. Lutein transport by Caco-2 TC-7 cells occurs partly by a facilitated process involving the scavenger receptor class B type I (SR-BI). *Biochem. J.* **387:** 455–461.

26. Reboul, E., A. Goncalves, C. Comera, R. Bott, M. Nowicki, J. F. Landrier, D. Jourdheuil-Rahmani, C. Dufour, X. Collet, and P. Borel. 2011. Vitamin D intestinal absorption is not a simple passive diffusion: evidences for involvement of cholesterol transporters. *Mol. Nutr. Food Res.* **55:** 691–702.

27. Goncalves, A., B. Gleize, R. Bott, M. Nowicki, M. J. Amiot, D. Lairon, P. Borel, and E. Reboul. 2011. Phytosterols can impair vitamin D intestinal absorption in vitro and in mice. *Mol. Nutr. Food Res.* **55(Suppl 2):** S303–S311.

28. Goncalves, A., B. Gleize, S. Roi, M. Nowicki, A. Dhaussy, A. Huertas, M. J. Amiot, and E. Reboul. 2013. Fatty acids affect micellar properties and modulate vitamin D uptake and basolateral efflux in Caco-2 cells. *J. Nutr. Biochem.* **24:** 1751–1757.

29. Kartz, G. A., R. L. Holme, K. Nicholson, and D. Sahoo. 2014. SR-BI/CD36 chimeric receptors define extracellular subdomains of SR-BI critical for cholesterol transport. *Biochemistry.* **53:** 6173–6182.

30. Mansbach 2nd, C. M., R. S. Cohen, and P. B. Leff. 1975. Isolation and properties of the mixed lipid micelles present in intestinal content during fat digestion in man. *J. Clin. Invest.* **56:** 781–791.

31. Spivak, W., C. Morrison, D. Devinuto, and W. Yuey. 1988. Spectrophotometric determination of the critical micellar concentration of bile salts using bilirubin monoglucuronide as a micellar probe. Utility of derivative spectroscopy. *Biochem. J.* **252:** 275–281.

32. Morita, S. Y., A. Kobayashi, Y. Takanezawa, N. Kioka, T. Handa, H. Arai, M. Matsuo, and K. Ueda. 2007. Bile salt-dependent efflux of cellular phospholipids mediated by ATP binding cassette protein B4. *Hepatology.* **46:** 188–199.

33. DeLong, L. J., and J. W. Nichols. 1996. Time-resolved fluorescence anisotropy of fluorescent-labeled lysophospholipid and taurodeoxycholate aggregates. *Biophys. J.* **70:** 1466–1471.

34. Reboul, E., Z. Soayfane, A. Goncalves, M. Cantiello, R. Bott, M. Nauze, F. Terce, X. Collet, and C. Comera. 2012. Respective contributions of intestinal Niemann-Pick C1-like 1 and scavenger receptor class B type I to cholesterol and tocopherol uptake: in vivo v. in vitro studies. *Br. J. Nutr.* **107:** 1296–1304.

35. Rigotti, A., S. L. Acton, and M. Krieger. 1995. The class B scavenger receptors SR-BI and CD36 are receptors for anionic phospholipids. *J. Biol. Chem.* **270:** 16221–16224.

36. Kawasaki, Y., A. Nakagawa, K. Nagaosa, A. Shiratsuchi, and Y. Nakanishi. 2002. Phosphatidylserine binding of class B scavenger receptor type I, a phagocytosis receptor of testicular Sertoli cells. *J. Biol. Chem.* **277:** 27559–27566.

37. Drover, V. A., D. V. Nguyen, C. C. Bastie, Y. F. Darlington, N. A. Abumrad, J. E. Pessin, E. London, D. Sahoo, and M. C. Phillips. 2008. CD36 mediates both cellular uptake of very long chain fatty acids and their intestinal absorption in mice. *J. Biol. Chem.* **283:** 13108–13115.

38. Neculai, D., M. Schwake, M. Ravichandran, F. Zunke, R. F. Collins, J. Peters, M. Neculai, J. Plumb, P. Loppnau, J. C. Pizarro, et al. 2013. Structure of LIMP-2 provides functional insights with implications for SR-BI and CD36. *Nature.* **504:** 172–176.

39. Rojo-Martinez, G., F. J. Soriguer, S. Gonzalez-Romero, F. Tinahones, F. Moreno, S. R. de Adana, M. J. Garriga, I. Esteva, J. Garcia-Arnes, J. M. Gomez-Zumaquero, et al. 2000. Serum leptin and habitual fatty acid dietary intake in patients with type 1 diabetes mellitus. *Eur. J. Endocrinol.* **142:** 263–268.